Journal of Solid State Chemistry **156,** 445–451 (2001)
doi:10.1006/jssc.2000.9020, available online at http://www.idealibrary.com on IDEAL®

Suppression of Modulations in Fluorinated Bi-2201 Phases

J. Hadermann, N. R. Khasanova, and G. Van Tendeloo

EMAT, University of Antwerp (RUCA), Groenenborgerlaan 171, B-2020 Antwerp, Belgium

and

A. M. Abakumov, M. G. Rozova, A. M. Alekseeva, and E. V. Antipov

Department of Chemistry, Moscow State University, 119899 Moscow, Russia

Received August 16, 2000; in revised form October 12, 2000; accepted October 27, 2000

$Bi_2Sr_{1.6}La_{0.4}CuO_{6.33}$ and $Bi_2Sr_{1.2}La_{0.8}CuO_{6.46}$ are fluorinated using XeF_2 as a fluorinating agent and studied by X-ray powder diffraction and high-resolution electron microscopy. The highly fluorinated Bi-2201 phase undergoes a structural transformation that is accompanied by the formation of an *I*-centered tetragonal unit cell, the suppression of the $\sqrt{2}a_p \times \sqrt{2}a_p$ superstructure, the disappearance of the $(BiO)_2$ modulation, and an elongation of the *c* parameter of about 1.65–1.77 Å. The modification of the Bi_2O_2 block into a $Bi_2O_{2-\delta}F_{2+\delta}$ block with filled tetrahedral interstitial positions is responsible for the observed structural changes and eliminates the mismatch between the (BiO) rock salt layers and the perovskite (CuO_2) layers. The structure of the fluorinated material is compared with the structures of other intercalated Bi-based cuprates and phases composing $Bi_2(O,F)_4$ blocks in the structure.

Key Words: **fluorination; Bi-2201; $Bi_2Sr_{1.6}La_{0.4}CuO_{6.33-x}F_{2+x}$; $Bi_2Sr_{1.2}La_{0.8}CuO_{6.46}$; $Bi_2Sr_{1.6}La_{0.4}CuO_{6.33}$.**

1. INTRODUCTION

Among the different layered cuprates the bismuth cuprates, $Bi_2Sr_2Ca_{n-1}Cu_nO_{2n+4+\delta}$, exhibit a particular behavior. These oxides, which consist of an intergrowth structure, differ from the corresponding thallium bilayer cuprates by the presence of a strong modulation. The incommensurate modulation is believed to be caused by a mismatch between the (BiO) rock salt type layer and the perovskite (CuO_2) layers. The mismatch is reduced by the insertion of extra oxygen in the (BiO) layer and by the cooperative displacements of the Bi and O atoms from their ideal positions within this plane which enables the appropriate Bi coordination to occur (1, 2). However, this rearrangement of the $Bi_2O_{2+\delta}$ block affects the rest of the structure through the corrugation of the adjacent layers and leads to the appearance of strong satellite reflections observed by different diffraction methods. The inserted oxygen provides holes to the conduction band contributing thereby to the superconductivity. For compounds of a given cation composition the amount of extra oxygen, the δ value, can be varied in a limited range depending on the synthesis conditions (3, 4). These parameters appear to be crucial for the phase stability and for the superconducting properties of the Bi-2201 phase. Monophasic samples with a partial substitution of Bi for Sr, $Bi_{2+x}Sr_{2-x}CuO_{6+\delta}$ are not superconducting, but superconductivity can be induced by rare earth doping on the Sr site. The parabolic-like compositional dependence of T_c with a maximum of 33 K at $x = 0.4$ was observed in a $Bi_2Sr_{2-x}La_xCuO_{6+\delta}$ solid solution (4). On further La doping T_c decreases and for $Bi_2Sr_{1.3}La_{0.7}CuO_{6+\delta}$ the superconductivity disappears. The suppression of superconductivity at a higher La content was assigned to the reduction of the Cu oxidation state upon heterovalent substitution, and attempts to oxidize further by oxygen treatments were unsuccessful.

Fluorination was successfully explored for oxidizing different cuprates, and several new superconducting compounds were prepared (5, 6). In contrast to the anion exchange of F^- for O^{2-}, which reduces the copper oxidation state, fluorine intercalation on the interstitial site leads to the oxidation of the conducting (CuO_2) planes and, in several cases, to structural transformations (5, 6, 17). It is of interest to examine the possibility of further oxidation of the Bi-based cuprates by fluorination and to study its effect on T_c. Considering the structural simplicity of the Bi-2201 phase and the strong effect of slight hole doping on its properties (since all holes correspond to one (CuO_2) plane) the fluorination of the Bi-2201 phase was attempted, and two compounds, the superconducting $Bi_2Sr_{1.6}La_{0.4}CuO_{6.33}$ and the non superconducting $Bi_2Sr_{1.2}La_{0.8}CuO_{6.46}$, were selected for this purpose.

0022-4596/01 $35.00

2. EXPERIMENTAL

The initial compounds, $Bi_2Sr_{1.6}La_{0.4}CuO_{6.33}$ and $Bi_2Sr_{1.2}La_{0.8}CuO_{6.46}$, were prepared by a ceramic method using Bi_2O_3, $SrCO_3$, CuO, and La_2O_3 as starting materials. Stoichiometric amounts of these materials were mixed, pressed into pellets, and heated at 720, 800, 850, and 870°C with subsequent regrinding for 100 h. The X-ray diffraction patterns are indexed in the *Amaa* space group with cell parameters $a = 5.398(2)$ Å, $b = 5.368(1)$ Å, $c = 24.349(4)$ Å and $a = 5.439(4)$ Å, $b = 5.422(2)$ Å, $c = 24.00(1)$ Å for the first and second compound, respectively. $Bi_2Sr_{1.6}La_{0.4}CuO_{6.33}$ demonstrates a superconducting transition with a T_c of 27 K and no superconductivity is detected for $Bi_2Sr_{1.2}La_{0.8}CuO_{6.46}$. The observed parameters as well as the oxygen content, determined by iodometric titration, agree with the previously published data (1, 4).

The initial compounds (0.3 g) were mixed with XeF_2 (provided by the Laboratory of Inorganic Synthesis of the Institute of Applied Chemical Physics "Kurchatovskii Institut," Moscow, Russia) in molar ratios of 1:1, 1:1.5, and 1:3 and ground in an agate mortar. All the operations with XeF_2 were carried out in a glove box filled with dried N_2. The mixtures were then placed in a Ni crucible and sealed in an N_2-filled copper tube. Different fluorinated samples were prepared by annealing at 150 and 200°C for 15 h and at 300°C for 40 and 80 h and subsequently furnace cooling to room temperature.

The phase composition of the samples and the lattice parameters of the compounds were determined by X-ray diffraction using a focusing Guinier camera FR-552 (Cu$K\alpha_1$ radiation, germanium internal standard). The formal copper valence of the pure samples was determined by iodometric titration.

The ac susceptibility measurements were carried out in the temperature range of 12–100 K at an external field amplitude of 1 Oe and a frequency of 27 Hz.

Electron diffraction (ED) and high resolution electron microscopy (HREM) were performed with a JEOL 4000EX microscope. The image simulations were made using the MacTempas software. The electron diffraction X-ray (EDX) analysis and electron diffraction were performed using a Philips CM20 microscope with a LINK-2000 attachment. The presence of fluorine in the samples was checked qualitatively since an exact quantitative determination of the fluorine content was difficult due to the low Z number.

3. RESULTS

The fluorination conditions and the cell parameters of the obtained compounds are given in Table 1. In several cases, particularly for $Bi_2Sr_{1.2}La_{0.8}CuO_{6.46}$, the fluorination results in a partial decomposition of the initial compounds with the release of badly crystallized LaOF, SrF_2, BiOF, and BiF_3 detected by X-ray diffraction. Due to the presence of broad reflections corresponding to the admixture phases the characterization of these samples by X-ray diffraction is difficult and they were not investigated further.

For all the fluorinated samples the temperature dependence of the magnetic susceptibility was measured and no superconducting transition down to 12 K was detected in any of them.

The X-ray patterns of $Bi_2Sr_{1.6}La_{0.4}CuO_{6.33}$ fluorinated at 150 and 200°C (samples 2 and 3) indicate the presence of two phases in both samples. While the first phase (A) is identified as similar to the initial compound with slightly modified cell parameters, a significant structural transformation occurs for the second phase (B). Its lattice parameters are determined as $a \approx b \approx 3.8$ Å and $c \approx 26$ Å, indicating a considerable expansion along the c axis (about 1.6–1.8 Å) with a simultaneous suppression of the $\sqrt{2}$ superstructure in the a–b plane. A significant amount of the B phase is found in both samples.

TABLE 1
Fluorination Conditions and Cell Parameters for the Initial and Fluorinated Compounds

No.	Fluorination conditions		a(Å)	b(Å)	c(Å)	V_{Cu}
1	$Bi_2Sr_{1.6}La_{0.4}CuO_{6.33}$		5.398(2)	5.368(1)	24.349(4)	2.25
2	1:1 XeF_2; 15 h at 150°C	A	5.419(1)	5.381(1)	24.370(9)	
		B	3.858(3)	3.832(3)	25.99(3)	
3	1:1 XeF_2; 15 h at 200°C	A	5.418(1)	5.3802(9)	24.406(6)	
		B	3.837(1)		26.18(2)	
4	1:1.5 XeF_2; 40 h at 300°C		5.407(1)	5.407(1)	24.200(8)	2.16
5	1:3 XeF_2; 80 h at 300°C	*	5.410(2)	5.410(2)	24.26(1)	
6	$Bi_2Sr_{1.2}La_{0.8}CuO_{6.46}$		5.430(4)	5.422(2)	24.00(1)	2.12
7	1:1.5 XeF_2; 40 h at 300°C		5.432(1)	5.432(1)	24.07(1)	2.05
8	1:1 XeF_2; 15 h at 150°C	*	5.430(1)	5.430(1)	24.15(1)	

*Decomposition products were detected on X-ray diffraction patterns.

For both initial compounds the fluorination at 300°C for 40 h produces almost pure samples (Nos. 4 and 7). Their X-ray patterns are similar to those of the starting materials and are indexed in the *Amaa* space group, with slightly modified cell parameters. It should be pointed out that in several cases (samples 4, 5, 7, and 8) a pseudotetragonal unit cell was considered, but the actual symmetry of these phases is orthorhombic due to the modulation, the presence of which was confirmed by electron microscopy and is described later. The iodometric titration reveals the reduction of the copper oxidation state for both sample 4 (from $V_{cu} = +2.25$ to $+2.16$) and sample 7 (from $V_{cu} = +2.12$ to $+2.05$). The fluorination at 300°C for a longer time (80 h) results in the decomposition of $Bi_2Sr_{1.2}La_{0.8}CuO_{6.46}$, while for $Bi_2Sr_{1.6}La_{0.4}CuO_{6.33}$ (sample 5) it leads only to small changes in the cell parameters and to the appearance of some decomposition products.

The structure characterization of the fluorinated compounds by X-ray diffraction is complicated because in several cases the samples contain two phases, and the overlapping of some reflections due to the similar subcells is unavoidable. The presence of the satellites caused by the modulation adds even more difficulties to this investigation. To resolve these problems, the samples 2–4 and 7 were studied by electron microscopy. Moreover HREM can provide information about the structure modulation which is difficult to elucidate from X-ray diffraction only.

The transmission electron microscopy (TEM) study of samples 2 and 3 confirms the presence of two different phases (A and B) in these samples. The ED patterns taken from the A phase are similar to those of the initial compound: the basic spots compatible with the *Amaa* space group are accompanied by satellite reflections. Figure 1 represents a [010]* ED pattern of the A phase together with the corresponding HREM image where the corrugation of the layers caused by the modulation can be seen. The modulation vector $\boldsymbol{q} = 0.23a^* + 0.7c^*$, estimated from the ED patterns, is rather close to that of the initial compound. The EDX analysis reveals a small amount of fluorine in the crystallites of the A phase (Fig. 2A), confirming thereby that the small changes in the unit cell parameters found by X-ray diffraction are due to the fluorination.

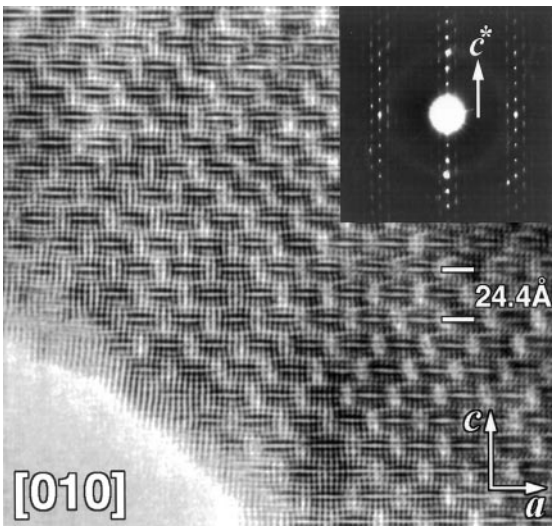

FIG. 1. [110] HREM image for the A phase of $BI_2Sr_{1.6}La_{0.4}Cu(O,F)_x$ (sample 2). The corresponding ED pattern is shown as an inset.

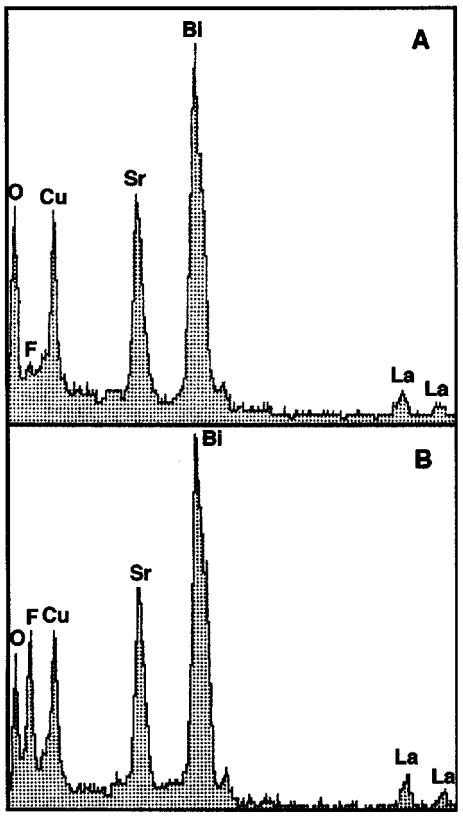

FIG. 2. Parts of the EDX spectrums of the A phase (A) and the B phase (B) (sample 2), showing the F($K\alpha$) peak in the low energy range.

The ED patterns of the B phase (Fig. 3) show that it has a unit cell with $a \approx b \approx 3.8$ Å and $c \approx 26.0$ Å, which agrees well with the X-ray diffraction data. No satellite reflections and no additional reflections that might correspond to a $\sqrt{2}a_p$ superstructure are observed on any of ED patterns. The reconstruction of the reciprocal lattice using sets of ED patterns from several crystals reveals the extinction conditions $hkl: h + k + l = 2n$, compatible with a body-centered space group. Thus, for the fluorinated material of the B phase, the space group $I4/mmm$ can be chosen for the tetragonal phase (sample 2) and $Immm$ for the orthorhombic one (sample 3). The transformation relations between the initial and the new unit cell are given by $[110]^* = [100]^*_I$, $[1\bar{1}0]^* = [010]^*_I$, where I denotes the new, I-centered unit cell. The EDX analysis does not reveal any changes in the

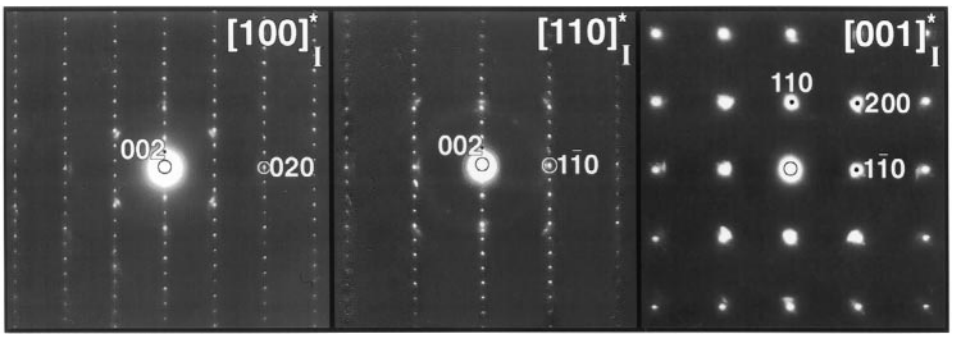

FIG. 3. Electron diffraction patterns taken along the main zones of the B phase (sample 2).

cation composition of the B phase, but, contrary to the A phase, a large amount of fluorine is detected in the structure (Fig. 2B).

Phase B is unstable and decomposes under an intense electron beam. This does not affect the recording of the diffraction patterns, but severely hinders the acquisition of HREM images. To avoid these problems we attempted a low-dose technique that suggests the use of the spread beam with long exposure times. The HREM images of the B phase taken in this way confirm the results of the reciprocal space investigation. The HREM image along the $[110]_I$ direction shown in Fig. 4 presents a modulation-free layered crystal structure with the positions of the (BiO) layers indicated by arrows. According to the image simulation the Bi atoms correspond to the dark spots in these rows. From the HREM image along $[100]_I$ given in Fig. 5 one can see that the staggered configuration of the $(BiO)_2$ layers is maintained.

From the TEM investigation of samples 4, 5, and 7 no remarkable changes in the structures of the fluorinated phases are observed. Their ED patterns are rather similar to the corresponding patterns of the initial compounds, but small amounts of fluorine detected by the EDX analysis suggest that the changes in the cell parameters are caused by the fluorination.

4. DISCUSSION

Previous studies demonstrated that the fluorination of cuprates involves different reactions. The oxidation of the (CuO_2) planes results from the intercalation of fluorine into a structure that contains either anion vacancies or interstices suitable for the accommodation of fluorine. Another competing reaction taking place during the fluorination is an anion exchange, i.e. the replacement of oxygen atoms by fluorine. It may lead either to the partial reduction of Cu if one O^{2-} ion is replaced by one F^- ion (a reaction of type I) or, if one O^{2-} is replaced by two F^-, to the increase of the overall amount of anions in the structure without changing the Cu oxidation state (a reaction of type II). The inner walls of the Cu tube, which is used as a reaction vessel, adsorb the released oxygen. Usually both kinds of anion exchange reactions occur simultaneously at high temperatures (350–500°C), while at low temperatures (150–300°C) the insertion process dominates (5, 17).

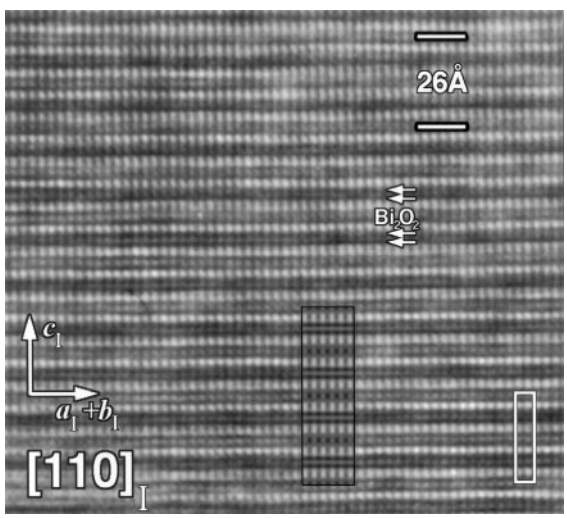

FIG. 4. HREM image of the B phase taken along $[110]_I$. The inset shows the corresponding calculated image ($\Delta f = -115$ nm, $t = 9$ nm). The arrows indicate the (BiO) layers.

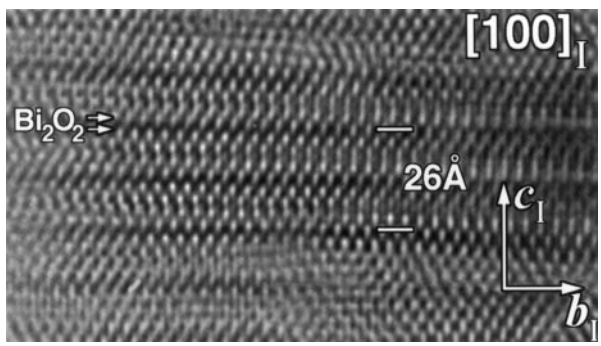

FIG. 5. $[100]_I$ HREM image of the B phase (sample 2). Positions of the (BiO) layers are indicated by arrows and confirm the staggered configuration of these layers.

The fluorination of the Bi-2201 phase appears to follow the anion exchange reaction, even if the fluorination temperature is rather low (150–200°C). All the fluorinated materials exhibit unit cells that are expanded in the *a*–*b* plane in comparison with the cell dimensions for the initial non-fluorinated phases, thus reflecting the reduction of the Cu atoms due to reaction I. Indeed, the decrease in the formal Cu valence is supported for samples 4 and 7 by the results of the iodometric titration. The low formal Cu valence can also provide an explanation for the absence of superconductivity in the fluorinated Bi-2201 phases. Another possible explanation for the absence of superconductivity could be that Bi is oxidized rather than copper, and superconductivity is eliminated due to charge redistribution. For the highly fluorinated B phase the significant modification of the structure can be attributed to the insertion of a considerable amount of fluorine by reaction II. A possible model for this transformation is drawn on the basis of the ED patterns and the HREM images of the B phase and the structure consideration of different Bi-containing compounds.

As a possible location for the introduced fluorine the position between the double (BiO) layers was considered. The bonding between these two layers is weak, and this position is subjected to various intercalations (I_2, Br_2, $HgBr_2$, LiI_3) (7–11). Iodine incorporation into the structure of the Bi-2212 and Bi-2223 phases leads to an expansion along the *c* axis and changes the rock salt alternation of the (BiO) layers. The separation of the two (BiO) layers by the iodine layer results in the disappearance of the staggered configuration of the (Bi_2O_2) block, i.e., the loss of the relative shift of the (BiO) layers and the formation of a primitive unit cell. No serious effect on the modulation is observed due to the weak interaction between the (BiO) and the *I* layers, and only a small decrease in T_c is detected for the intercalated compounds (8).

For the B phase, fluorine insertion also results in a remarkable expansion along the *c* axis; however, the rock salt configuration of the (BiO) layers is maintained as shown by the *I*-centered space group and the HREM evidence. The disappearance of the modulations and of the $\sqrt{2}a_p \times \sqrt{2}a_p$ superstructure indicates that the inserted fluorine significantly modifies the $Bi_2O_{2+\delta}$ block arrangement, eliminating the mismatch between the blocks. Fluorine is proposed to be accommodated between the (BiO) layers in the interstitial fluorite type positions tetrahedrally coordinated by four Bi^{3+} cations. To model this transformation we considered the structures of several compounds in which Bi is coordinated by O and F, such as BiOF (12), BiF_3 (13), and Bi_2NbO_5F (14). The structure model comprising Bi cations in a capped square antiprism with four short Bi–F and five longer Bi–O distances (Fig. 7) was built using the cell parameters and the *Immm* space group derived from the ED patterns. In this coordination behavior the inserted fluorine forms a strong bond to Bi, which is accompanied by a rearrangement of this structural block, while the rest of the structure (the other interlayer distances) is comparable to the initial one. The proposed positions of fluorine, oxygen, and Bi in the transformed block are quite similar to those in the Aurivillius phase, Bi_2NbO_5F, and in BiOF, where the Bi coordination is a square antiprism with four Bi–F distances of 2.29 Å and four Bi–O distances of 2.71 Å (12, 14). Therefore, the Bi_2O_{2+x} block transforms into a $Bi_2O_{2-x}F_{2+x}$ block (if all anion positions are occupied, but most probably some of them are vacant) with the coordination described above. The comparison of the interlayer distances in the initial and the fluorinated Bi-2201 with those observed for the $Bi_2O_2F_2$ or Bi_2O_4 blocks in the Aurivillius-type phases (14, 15) allows us to unravel the structural reason for the unit cell expansion along the *c* axis upon the filling of the interstitial positions by extra anions. As shown in Fig. 6, the distance between the two Bi layers above and below the interstitial positions decreases from 3.18–3.20 Å in the non-fluorinated Bi-2201 to 2.49–2.56 Å in the Aurivillius phases (14, 15) due to the electrostatic interaction between the interstitial anions and the Bi^{3+} cations. On the other hand, the repulsion between the interstitial anions and the oxygen atoms in the (BiO) layers increases the distance between the oxygen atoms. In the initial Bi-2201 structure the (BiO) layers are nearly flat and the distance along the *c* axis between the Bi^{3+} and the oxygen atoms in this layer is in the range of 0.24–0.26 Å. This distance increases to 0.92–1.07 Å in the Aurivillius phases, overpowering the decrease in the separation between the Bi layers and resulting in the overall expansion of the whole block with 0.7–1 Å (from

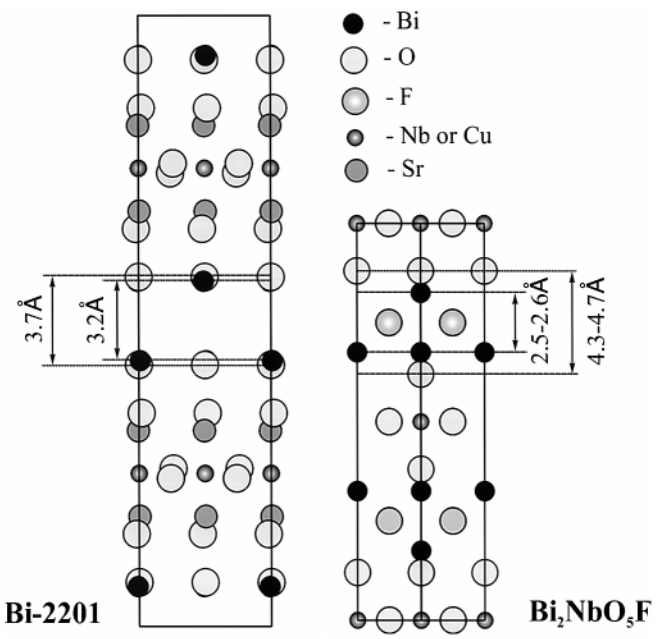

FIG. 6. Comparison of the interlayer distances in the Bi-2201 and Aurivillius phases (the structure of Bi_2NbO_5F is shown as an example).

3.66–3.72 Å to 4.32–4.7 Å). The thus expected value of the increase in the c parameter should be 1.4–2 Å, which agrees well with the experimentally observed value of 1.65–1.77 Å.

The structure proposed above (Fig. 7) is used for the image simulations (Fig. 4) and gives a good agreement with the experimental images. However, this structure should be regarded as only a rough model because the low scattering factors of O^{2-} and F^- and the small differences between them make it difficult to examine the distribution of oxygen and fluorine between the different anion positions or to determine their occupancies. The same arrangement of Bi and F was recently reported for the Bi-2223 compound fluorinated by NH_4HF_2 (16). In this case the fluorination also produced a mixture of two phases, and the structure of the fluorinated compound, $Bi_2Sr_2Cu_3O_8F_4$, was refined by the Rietveld method on the basis of neutron diffraction data. In the new compound fluorine was found to replace oxygen in the (BiO) layer in a 2:1 ratio, leading to a similar expansion (about 1.8 Å) along the c axis, but the disappearance of neither the $\sqrt{2}a_p \times \sqrt{2}a_p$ superstructure nor the modulation was mentioned.

The fluorination of the Bi-2201 phases leads not only to an increase in the thickness of the $Bi_2O_{2-x}F_{2+x}$ block but also to the expansion of this block in the a–b plane. This could be explained by the increased coordination number of the Bi atoms, followed by the elongation of the interatomic distances as well as by the repulsion forces between the anions. As a result, the mismatch between the (BiO) rock salt type layer and the perovskite (CuO_2) layers is no longer existent, leading to the suppression of the modulations in the structure of the highly fluorinated Bi-2201 phases.

In contrast to the case of fluorination, the intercalation of iodine has a different effect on the structure of the Bi-containing cuprates, which could be explained by the differences in their size and electronegativity. The smaller fluorine ($r(F^-) = 1.19$ Å) is located between the double (BiO) layers in the tetrahedra of four Bi atoms and forms strong bonds modifying this block. However, the larger size of I^- ($r(I^-) = 2.20$ Å) requires the formation of a polyhedron with a larger coordination number and with longer interatomic Bi–I distances. In the phase with the ideal $IBi_2Sr_2Ca_2Cu_3O_x$ composition [8], iodine is located in a square prism of Bi atoms with Bi–I separations of 4.07–4.22 Å. These distances are even longer than the Cs–I separation in the CsI structure (ICs_8 cubes with d(Cs–I) = 3.96 Å) showing that the Bi–I bond has a weak van der Waals interaction and does not significantly influence the structure or the dimensions of the (BiO) layers.

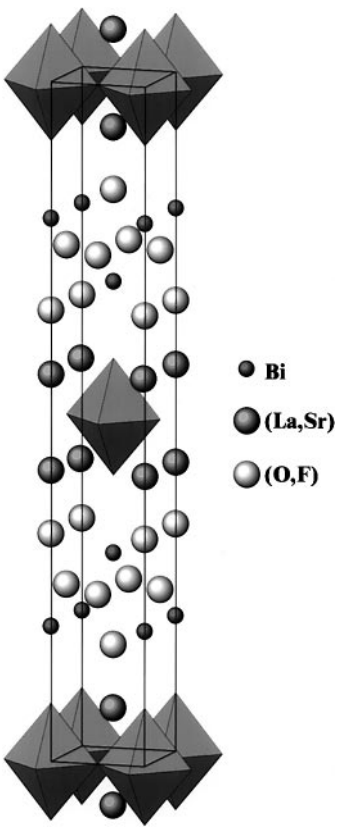

FIG. 7. Structure model of the highly fluorinated B phase used for image simulations.

ACKNOWLEDGMENTS

This work was performed in the framework of IUAP-PAI 4/10 of the Belgian government and was partially supported by INTAS-99-1136 and Volkswagen Grant I/75849.

REFERENCES

1. H. W. Zandbergen, W. A. Groen, F. C. Mijlhoff, G. Van Tendeloo, and S. Amelinckx, *Phys. C* **156,** 325–354 (1988).
2. Y. Le Page, W. R. McKinon, J.-M. Tarascon, and P. Barboux, *Phys. Rev. B* **40,** 6810–6816 (1989).
3. R. M. Fleming, S. A. Sunshine, L. F. Shnemeyer, R. B. VanDover, R. J. Cava, P. M. Waszak, S. H. Glarum, and S. M. Zahurak, *Phys. C* **173,** 37–50 (1991).
4. N. R. Khasanova and E. V. Antipov, *Phys. C* **246,** 241–252 (1995).
5. A. M. Abakumov, J. Hadermann, G. Van Tendeloo, R. V. Shpanchenko, P. N. Oleinikov, and E. V. Antipov, *J. Solid State Chem.* **142,** 440–450 (1999).
6. M. Al-Mamouri, P. P. Edwards, C. Greaves, and M. Slaski, *Nature* (*London*) **369,** 382–383 (1994).
7. X.-D. Xiang, S. Mckernan, W. A. Vareka, A. Zettl, J. L. Corkill, T. W. Barbee, III, and M. L. Cohen, *Nature* **348,** 145 (1990).
8. N. Kijima, R. Gronsky, X.-D. Xiang, W. A. Vareka, J. Hou, A. Zettl, J. L. Corkill, and M. L. Cohen, *Phys. C* **198,** 309–317 (1992).
9. S.-J. Hwang, N.-G. Park, D.-H. Kim, and J.-H. Choy, *J. Solid State Chem.* **138,** 66 (1998).
10. X.-D. Xiang, A. Zettl, W. A. Vareka, J. L. Corkill, T. W. Barbee, III, and M. L. Cohen, *Phys. Rev. B* **43,** 11,496 (1991).
11. T. Kijima, H. Sushida, M. Yada, and M. Machida, *J. Solid State Chem.* **141,** 452 (1998).
12. J. L. Soubeyroux, S. F. Matar, J. M. Reau, and P. Hagenmuller, *Solid State Ionics* **14,** 337 (1984).

13. A. K. Cheetam and N. Norman, *Acta Chem. Scand.* **28,** 55 (1974).
14. B. Aurivillius, *Ark Kemi* **5,** 519 (1952).
15. A. D. Rae, J. G. Thompson, and R. L. Withers, *Acta Crystallogr. B* **47,** 870 (1991).
16. E. Bellingeri, G. Grasso, R. E. Gladyshevskii, M. Dhalle, and R. Flukiger, *Phys. C* **329,** 267 (2000).
17. J. Hadermann, A. M. Abakumov, O. I. Lebedev, G. Van Tendeloo, M. G. Rozova, R. V. Shpanchenko, B. Ph. Pavljuk, E. M. Kopnin, and E. V. Antipov, *J. Solid State Chem.* **147,** 647–656 (1999).